A density functional theory study on the binding of NO onto FePc films

Ngoc L. Tran[a] and Andrew C. Kummel
Department of Chemistry and Biochemistry, University of California, San Diego, La Jolla, California 92039-0358, USA

(Received 27 June 2007; accepted 22 September 2007; published online 4 December 2007)

To develop an atomistic understanding of the binding of NO with iron phthalocyanine (FePc), the interaction between NO (an electron withdrawing gas) and NH_3 (an electron donating gas) with an isolated FePc molecule (monomer) was compared with density functional theory. The simulations show that NO strongly chemisorbs to the Fe metal and physisorbs to all the nonmetal sites. Additionally, when NO physisorbs to the inner ring nitrogens, NO subsequently undergoes a barrierless migration to the deep chemisorption well on the Fe metal. Conversely, NH_3 only weakly chemisorbs to the Fe metal and does not bind to any other sites. Projected density of states simulations and analysis of the atomic charges show that the binding of NO to the FePc metal results in a charge transfer from the Fe metal to the NO chemisorbate; the opposite effect is observed for the binding of NH_3 to the Fe metal. Simulations of NO binding to the Fe metal of a monolayer FePc film and FePc trimer were also performed to show that intermolecular FePc-FePc interactions have a negligible effect on the FePc electronic structure and NO binding. © *2007 American Institute of Physics*. [DOI: 10.1063/1.2799988]

I. INTRODUCTION

Metallophthalocyanines (MPcs) are square planar molecules that can form highly ordered, chemically inert, and thermally stable films. They have been extensively studied with both experimental (photoemission spectroscopy,[1] reflection high-energy electron diffraction,[2] low-energy electron diffraction,[3] and scanning tunneling microscopy[4–6]) and theoretical [Hartree-Fock[7] and density functional theory (DFT)[8,9]] techniques. Their electronic and absorption properties can be modified by varying the metal center or adding ligands onto the organic rings making them an attractive candidate for use in chemical sensors.[10,11] Jones *et al.* showed that two-terminal resistive sensors with different *p*-type MPc films (CoPc, CuPc, NiPc, FePc, and ZnPc) could be used to discriminate between different electron accepting and electron donating gases at low ppm concentrations.[12] In addition, Tada *et al.* showed that *n*-type $CuPcF_{16}$-based organic field-effect transistors were highly sensitive to NH_3.[13]

Although the experimental and theoretical literature pertaining to MPc sensor applications is extensive, a basic understanding of gas chemisorption onto these metal coordination complexes is lacking. Existing theoretical investigations of MPcs have focused primarily on the electronic structure of the monomer,[7,14,15] the film in its β-crystalline form,[16] and the molecular interaction of the monomer with a substrate.[17] A few computational studies have investigated the interaction of an analyte with the MPc but did not allow the MPc-analyte complex to relax geometrically.[18,19] Of the studies that did allow for geometric relaxation, the focus was on analyte binding to the hydrogen bridge of the metal-free phthalocyanine.[20] When analyte binding to the metal-containing phthalocyanine was studied, site specific binding to the organics was not included.[21]

In the current study, DFT calculations were used to investigate the site specific interaction of NO and NH_3 with FePc monomer, trimer, and monolayer films. Analyte binding to the aromatic rings as well as to the metal center of the MPc was investigated. The chemisorption energies for various binding sites on the FePc molecule were evaluated, and all systems were allowed to relax geometrically. The effect of analyte induced changes on the electronic structure of the FePc monomer was also explored. Simulations comparing the binding of NO to the FePc monomer versus the monolayer film were also performed to investigate the effect of planar interaction on FePc electronic structure and NO binding. To ensure that analyte interaction with the monomer is a reasonable model of analyte interaction with bulk films, NO binding to the FePc trimer was calculated as well.

II. COMPUTATIONAL METHODS

Geometry optimizations of all systems (the three FePc systems mentioned above, gas phase NO, gas phase NH_3, and NO and NH_3 adsorbed onto the three FePc systems) were performed using the Vienna *ab initio* simulation package,[22–24] a plane-wave DFT code with periodic boundary conditions. The DFT simulations were performed with the PW91 variety of the generalized-gradient approximation (GGA), using ultrasoft Vanderbilt pseudopotentials as supplied within VASP,[24–26] and a single **k** point (located at the gamma point). To check for saturation of the plane-wave basis, the kinetic energy cutoff was sampled at 50 eV increments from 300 to 600 eV for one test case: NH_3 binding to the Fe metal of the isolated, gas phase FePc molecule. While the binding energy difference between cutoff energies of 300

[a]Electronic mail: ngoctran@ucsd.edu.

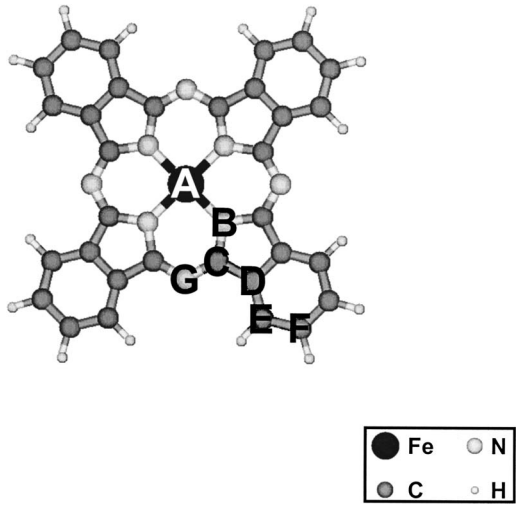

FIG. 1. Schematic of FePc monomer showing the seven binding sites investigated (A–G).

and 600 eV was more than 0.77 eV, the binding energy difference between cutoff energies of 400 and 600 eV was only 0.052 eV. In consideration of the large number of binding sites and binding configurations investigated in this study and the approximately three times computational time required for using the higher energy cutoff, the kinetic energy cutoff was set to 400 eV for simulations of all systems. All systems were geometrically relaxed to a convergence tolerance of 0.01 eV/Å. To account for the open-shell systems, spin polarization was also included in the simulations. The binding energies are calculated as

$$E_{\text{binding}} = E_{(\text{FePc+analyte})} - (E_{\text{FePc}} + E_{\text{analyte}}), \quad (1)$$

where $E_{(\text{FePc+analyte})}$ is the total energy of the FePc-analyte complex, E_{FePc} is the total energy of the FePc, and E_{analyte} is the total energy of the isolated NO or NH_3 analyte.

III. RESULTS AND DISCUSSION

A. NO and NH_3 binding to the FePc monomer

DFT simulations were used to calculate the binding energies of NO and NH_3 onto seven different sites listed as A through G on an isolated FePc molecule (Fig. 1). The isolated FePc molecule will be referred to as the monomer. The monomer was placed in a $20\times20\times15$ Å^3 tetragonal unit cell to ensure that interactions between FePc molecules in neighboring unit cells are negligible. The optimized FePc monomer has D_{4h} symmetry and simulated bond lengths and angles that agree with previous experimentally and computationally determined values to within 0.02 Å and 1°, respectively.[8,27] Since the binding energy for NO on the Fe metal of the monomer placed N end down was 0.94 eV more exothermic than for the O-end down case, binding to all other sites was studied using the N-end down configuration. This is a reasonable assumption considering that the N end of the NO radical contains the more reactive unpaired electron. In addition, numerous studies show an affinity for NO to bind to alkanes and aromatics through the nitrogen.[28,29]

TABLE I. Table of simulated binding energies for NO and NH_3 on the FePc monomer at all seven sites. The value reported for NO binding to site B is for the NO molecule prohibited from migrating to the Fe metal center.

Analyte binding sites	NO (eV)	NH_3 (eV)
Fe center (A)	−1.74	−0.37
Inner ring nitrogen (B)	−0.25	−0.01
Organic (C)	−0.20	−0.03
Organic (D)	−0.23	−0.02
Organic (E)	−0.23	−0.02
Organic (F)	−0.21	−0.02
Outer ring nitrogen (G)	−0.20	−0.03

Results of the DFT calculations for NO and NH_3 binding onto various sites on the monomer are summarized in Table I. For NO binding onto the Fe metal (site A), the calculations show that NO forms a strong bond to the metal with a well depth of −1.74 eV. The binding results in a N–Fe bond length of 1.71 Å and a nonplanar FePc molecule (Fig. 2). NO binding to the Fe metal causes the Fe metal to protrude from the FePc molecular plane toward the NO analyte while the organic rings buckle away from the analyte giving a N–Fe–N bond angle of 162° as compared to 180° for the clean monomer. NO placed on the carbons and nitrogens of the FePc molecule results in weakly bound physisorption ranging from −0.20 eV on the outer ring nitrogen (site G) to −0.23 eV on the organic ring (site D). When NO is placed on the inner ring nitrogen (site B), NO undergoes a barrierless migration from the inner ring nitrogen to the Fe metal in which the binding energy for the final Fe–NO configuration is −1.75 eV. When NO is placed on the inner ring nitrogen (site B) and restricted from migrating to the Fe metal by freezing the NO molecule in the x coordinate, NO still binds exothermically to the inner ring nitrogen site by −0.25 eV; this is the value for binding site B reported in Table I. In contrast to NO, NH_3 weakly chemisorbs via a nitrogen-end down configuration to the Fe metal (site A) with a modest well depth of −0.37 eV and does not bind to any other FePc site.

To better illustrate the role of the Fe metal and aromatics in NO binding, a potential energy surface diagram of NO binding onto the FePc monomer at various binding sites is shown in Fig. 3. The reaction coordinate was calculated

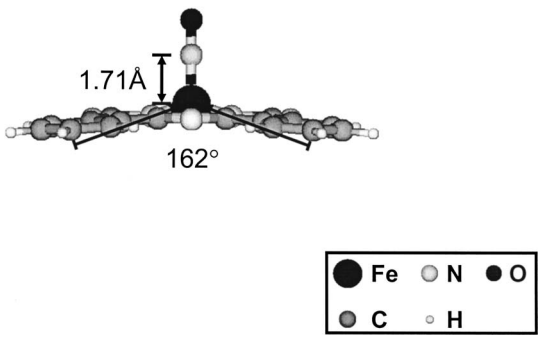

FIG. 2. Schematic of NO binding onto the metal center of the FePc monomer. The N–Fe–N bond angle changes from 180° to 162° upon NO chemisorption. The resulting Fe–N(O) bond length is 1.71 Å.

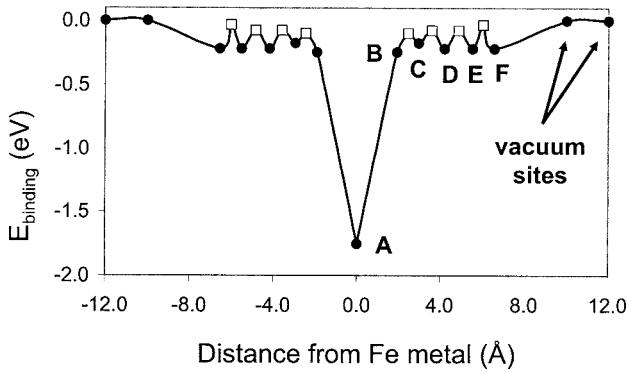

FIG. 3. Potential energy surface diagram of NO binding at various sites on the FePc monomer. Solid circles: binding energies for NO to Fe metal (A) and nonmetal physisorption sites (B–F). Open squares: barriers to diffusion from site to site. The line connecting the points acts only as a guide.

based on the distance from the binding site to the metal center. Note that the value reported for the inner ring nitrogen (site B) was calculated with NO frozen in the x coordinate so as to prevent NO from migrating onto the Fe metal. All other atoms were allowed to relax freely. Despite prohibiting the NO molecule from undergoing any lateral motion, NO binding onto site B still resides on the downward slope of the chemisorption well. These results show that NO can undergo a barrierless migration from site B to the Fe metal. In addition, barriers to migration from organic site to organic site (F to E, E to D, and D to C) and to the inner ring nitrogen site (C to B) were calculated by freezing the NO molecule at each halfway point between binding sites and allowing the FePc monomer to relax. As seen in Fig. 3, the barriers to migration from organic site to organic site and from organic site to the inner ring nitrogen site are on the order of 0.23 eV (F to E) to 0.11 eV (C to B) and, at temperatures above 77 K, can be easily overcome. In summary, NO can migrate with small barriers from the organic ring sites, suggesting that the FePc molecule acts to funnel NO to the deep chemisorption well on the Fe metal.

The simulated well depths suggest that NO binds weakly to the FePc organics and tightly to the FePc metal. This is consistent with a thermal desorption study where two peaks were observed for the nondissociative, molecular desorption of NO from a β-polymorph FePc powder.[30] The authors suggest that the high temperature peak corresponds to NO desorption from the Fe metal center. Based on Redhead's peak maximum method for first order desorption, the higher temperature desorption peak corresponds to an adsorption energy of 1.2 eV.[31] Note that hopping between sites is not taken into account in this model. In the case of NO on FePc, a multiple stage desorption path may exist whereby NO initially diffuses from the Fe metal and into the physisorption well on the organics. The DFT calculated barrier to diffusion from the Fe metal to the organics is about 1.5 eV, suggesting that the chemisorption energies predicted in this study are overestimated by 0.3 eV. The overestimation may be a result of the artificial, gross structural relaxation incurred by the isolated, single molecule FePc upon NO adsorption. However, this can be excluded because simulations of NO adsorption on a triple stack FePc, where gross structural relaxations are absent, predict binding energies that are very similar to the isolated monomer (see Sec. III C below). Most likely, the discrepancies observed in the DFT predicted and thermal desorption calculated adsorption energies are an artifact of the functional used in this study. Becke performed a comprehensive test of 55 systems and showed that for these tightly bound systems, GGA overbinds by 0.2 eV on average.[32] Despite the errors in these simulations, a qualitative conclusion can still be derived from these results where NO has a strong affinity to bind to the Fe metal as opposed to the organic ring but the organic rings act as precursor sites for chemisorption to the metal centers.

These simulated binding energies are also consistent with recent King and Wells sticking probability measurements for NO on a monolayer FePc on a Au(111) substrate.[33] The sticking experiments show that NO saturation occurs at 3% of a monolayer for various beam energies and surface temperatures. Since the metal represents about 3% of a monolayer, this is consistent with the DFT simulations described in this article showing chemisorption occurring only at the Fe metal. Additionally, the data show that the initial sticking probability (S_0) is large (40%) at low translational beam energy and low surface temperature. As the NO translational energy and surface temperature are increased, the initial sticking probability decreases linearly until at 300 K, S_0 is 0% for the highest beam energy. The monotonic decrease in sticking probability as surface temperature and incident beam energies are increased is consistent with NO trapping onto physisorption sites on the monolayer. These data are also consistent with the calculated well depths for NO binding onto the aromatics of the FePc monomer ($\sim$0.2 eV exothermic). Both the simulations and sticking data strongly suggest that NO adsorbs onto a monolayer FePc via multiple precursor-mediated physisorption pathways where it initially adsorbs onto the aromatics and subsequently diffuses and chemisorbs only onto the metal centers.

B. NO and NH_3 induced changes in the FePc monomer electronic structure

Many sensor studies have suggested that electron withdrawing gases (such as NO) inject holes into these p-type MPc films, thus increasing film current.[34] A study by Nyokong and Vilakazi showed that FePc modified electrodes gave the largest current increase upon NO oxidation when compared to the metal-free H_2Pc and various other metallated MPcs, suggesting that the NO and FePc interaction is strong.[35] The opposite effect is observed by electron donating gases (such as NH_3) where a decrease in film current is observed and attributed to trapped charge carriers.[36] An analysis of the total density of states (DOS) and projected density of states (PDOS) of the FePc monomer before and after NO and NH_3 adsorption onto the Fe metal shows that both analytes can induce a change in the FePc electronic structure. Since the states closest to the Fermi level (E_F) will most affect conductivity in the film, only the states in the energy range from −2.0 to 2.0 eV will be analyzed. The DOS of the FePc monomer prior to analyte adsorption [Fig.

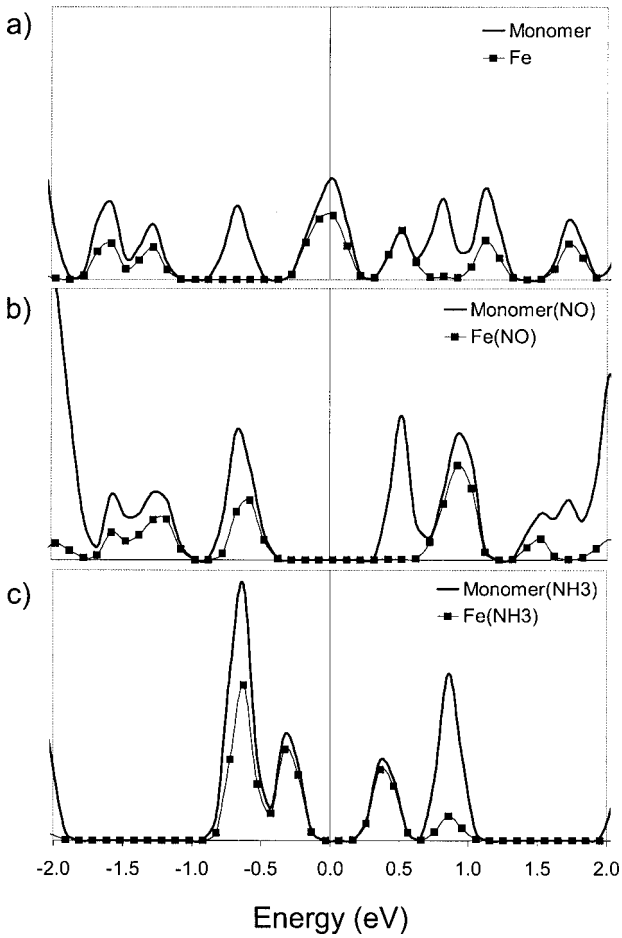

FIG. 4. Solid line represents FePc DOS and solid squares represent Fe projected DOS of the (a) clean FePc monomer, (b) NO adsorbed to the Fe metal of the FePc monomer, and (c) NH_3 adsorbed to the Fe metal of the FePc monomer.

4(a)] contains a partially filled state at the Fermi level (E_F) and an unfilled state centered at 0.53 eV. The Fe PDOS shows that these states are localized on the Fe atom. The presence of a partially filled state at E_F is also consistent with orbital-mediated tunneling spectroscopy measurements of CoPc and cobalt tetraphenylprophyrin, a Pc analog, on a Au(111) substrate whereby a midgap state exists for both organometallic films.[37] The Fe localized nature of this state suggests that FePc monolayer films are semiconducting, consistent with numerous sensing studies.[38]

NO binding to the Fe metal of the monomer [Fig. 4(b)] induces an obvious change in the monomer electronic structure. Upon NO chemisorption onto the Fe metal of the FePc monomer, the midgap Fe state is shifted into the filled state centered at −0.57 eV. The lowest energy unfilled Fe state shifts from 0.53 eV to the higher energy state at 0.93 eV. Upon NH_3 adsorption onto the Fe metal, Fig. 4(c) shows that the midgap Fe state at E_F is shifted into the filled state centered at −0.33 eV. The lowest energy unfilled Fe state shifts from 0.53 eV to the lower energy state at 0.43 eV. While the DFT calculations clearly show that NO and NH_3 adsorption to the Fe metal induces a change in FePc electronic structure, it is difficult to relate how these changes correspond to changes in MPc sensor response.

The PDOS of the clean FePc monomer for the nonequivalent carbon and nitrogen atoms also resembles that observed by Bialek *et al.* but is not discussed here since adsorption of either analyte at all carbon and nitrogen sites does not induce significant changes in these PDOSs.[39]

The analyte induced changes in MPc conductivity can be predicted from the calculated DOS by showing that charge transfer complexes are formed when electron withdrawing or electron donating gases interact with the MPc film.[10,11,40] An analysis of the atomic charges of the FePc monomer before and after NO and NH_3 adsorption using the Bader charge distribution method shows that charge transfer occurs between the adsorbate and FePc monomer.[41] Upon NO adsorption, the Fe metal loses $0.28e^-$ while the NO molecule gains $0.31e^-$, consistent with the electron withdrawing nature of NO. In contrast, the weak binding of NH_3 to the Fe metal results in a gain of $0.06e^-$ for the Fe metal and a loss of $0.07e^-$ for the NH_3 molecule, also consistent with the electron donating nature of NH_3. For both analytes, only a slight transfer of charge was observed for binding onto the nonmetal sites (less than $\pm 0.03e^-$). This is expected since the simulations show that NO only weakly binds to the nonmetal sites and NH_3 only binds to the metal. The calculated charge transfer is consistent with experimental results showing that NO increases while NH_3 decreases the current in *p*-type MPc films.[12,42]

C. NO binding to the Fe metal of the FePc trimer

To investigate the effect of out-of-plane FePc-FePc intermolecular interactions on the FePc electronic structure and analyte binding, simulations of NO sticking to the Fe metal of an FePc triple stack were performed. NO binding only to the Fe metal site of this system was investigated since NO binding to the Fe metal of the FePc monomer gave the greatest analyte-FePc interaction. In addition, binding to the metal center should be most perturbed by FePc-FePc out-of-plane interactions.

The adsorption energy of NO onto the Fe metal of a triple stack FePc was calculated. The triple stack FePc system will be referred to as the FePc trimer, and a schematic of this system can be found in Fig. 5(a). The FePc trimer was placed in a $20 \times 20 \times 15$ Å^3 tetragonal unit cell to ensure that interactions between FePc molecules in neighboring unit cells are negligible. FePc-FePc z spacing in the trimer was set to 3.4 Å and the N–Fe–N bond angle for all three FePc layers was 180° prior to relaxation, in accordance with experimentally determined values.[38,43] The bottom FePc layer of the trimer was geometrically frozen to imitate FePc in the bulk. The relaxed trimer had average simulated Fe-Fe and phenyl-phenyl z spacings of 3.44 and 3.50 Å, respectively [Fig. 5(a)]. These values resemble the experimentally determined value of 3.4 Å, suggesting that the FePc trimer is a good model of a thick FePc film.

A double stack FePc system (dimer) was also calculated where both the top and bottom FePc layers were allowed to relax. The dimer resulted in simulated Fe–Fe and phenyl-phenyl z spacings and bond angles that differ from the experimentally determined values by more than 30%, suggest-

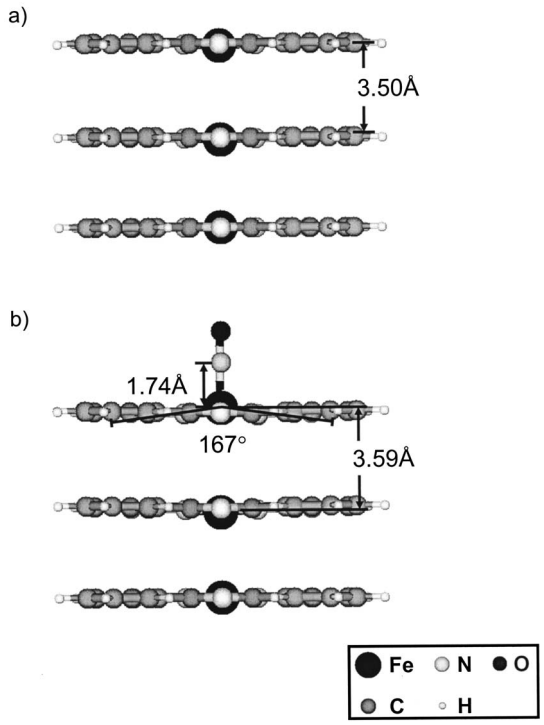

FIG. 5. Schematic of (a) the relaxed FePc trimer and (b) NO binding to the Fe metal of the FePc trimer. NO binding to the Fe metal gives a N–Fe–N bond angle and Fe–N(O) bond length of 167° and 1.74 Å, respectively.

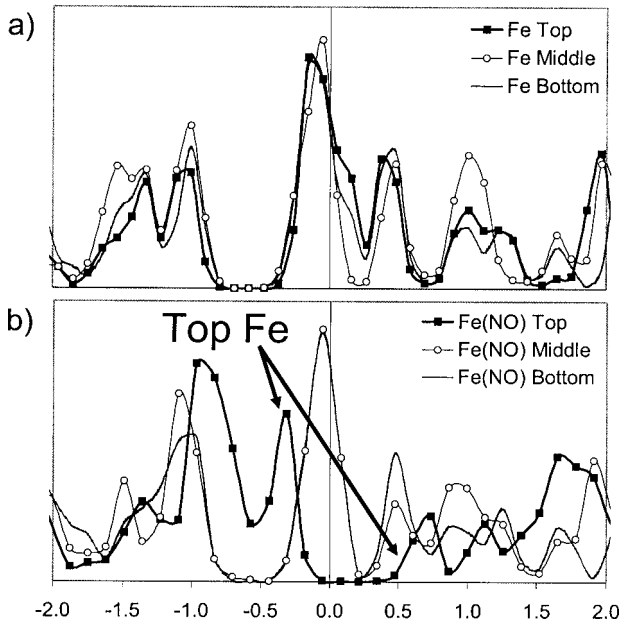

FIG. 6. Solid squares, open circles, and shaded line represent Fe PDOS of the top, middle, and bottom FePc, respectively, for the (a) clean FePc trimer and (b) NO adsorbed to the Fe metal of the trimer.

ing that the FePc dimer may not be the most appropriate system to model a thick FePc film. Since the FePc dimer is a poor model of a multilayer FePc film, NO binding to the Fe metal of the dimer will not be discussed.

The simulations show that NO adsorption to the Fe metal of the trimer is similar to NO adsorption to the Fe metal of the monomer. NO adsorption to the Fe metal of the trimer results in a well depth of −1.67 eV, which is nearly equivalent to NO adsorption to the monomer metal center. Analogous to the monomer calculation, the trimer calculations show that NO binding to the topmost Fe causes the Fe metal to protrude out of the FePc molecular plane [Fig. 5(b)] resulting in an Fe–N(O) bond distance of 1.74 Å and N–Fe–N bond angle of 167°. However, unlike NO binding to the monomer, the organic rings in the top layer of the trimer do not buckle away from the analyte. Most likely, interactions with the organics in the middle and bottom layers of the trimer prohibit the top organic layer from bending away from the analyte. This results in an average phenyl-phenyl z spacing of 3.54 Å. In addition, the average Fe–Fe z spacing has increased marginally to 3.59 Å.

Similar to the FePc monomer, chemisorption of NO onto the Fe metal of the FePc trimer induces a change in its electronic structure. Figure 6(a) shows the Fe PDOS of each layer of FePc labeled as top, middle, and bottom before NO adsorption onto the Fe metal of the top FePc layer. The Fe PDOSs of the individual layers in the trimer closely resemble that observed in the monomer where all three layers contain a partially filled Fe state at midgap and an unfilled Fe state in the conduction band at 0.48 eV. Similarity in the Fe PDOSs of the monomer and trimer suggests that Fe–Fe interactions in thick FePc films are small. As seen in Fig. 6(b), binding of NO to the Fe metal of the top FePc layer results in an electronic structure change similar to that observed in the FePc monomer but this change is confined to the Fe metal of the top FePc layer. The midgap Fe state is shifted into the filled state centered at −0.31 eV. The lowest energy unfilled state is shifted from 0.42 eV to the higher energy state at 0.73 eV. The PDOS of the Fe metal for the FePc middle and bottom layers remain relatively unchanged after NO adsorption, suggesting that FePc-FePc interactions are weak and do not significantly affect binding to the metal center. Again, the highly localized nature of the Fe PDOSs in the trimer strongly suggests that MPc films are semiconducting, consistent with numerous experimental studies.

Analysis of the atomic charges of the FePc trimer before and after NO adsorption onto the Fe metal using the Bader charge distribution method shows that there is a transfer of charge between the adsorbate and FePc trimer. When NO adsorbs onto the Fe metal, the Fe metal directly interacting with NO loses $0.26e^-$ while the NO molecule gains $0.27e^-$. This oxidation of the Fe metal is consistent with experimental results showing that NO increases the current in p-type MPc films. Additionally, these values are comparable to that observed for the FePc monomer and further suggest that out-of-plane FePc-FePc intermolecular interactions do not affect NO binding.

D. NO binding to the Fe metal of the FePc monolayer film

To investigate the effect of FePc-FePc in-plane interactions, the adsorption energy of NO onto the Fe metal of an FePc monolayer film was calculated. A schematic of the monolayer film is shown in Fig. 7(a). The monolayer film was placed in a $13.7\times13.7\times15$ Å^3 tetragonal unit cell and was modeled based on a monolayer FePc on a $23\times\sqrt{3}$ Au(111) surface.[5] The Au substrate was not included in these

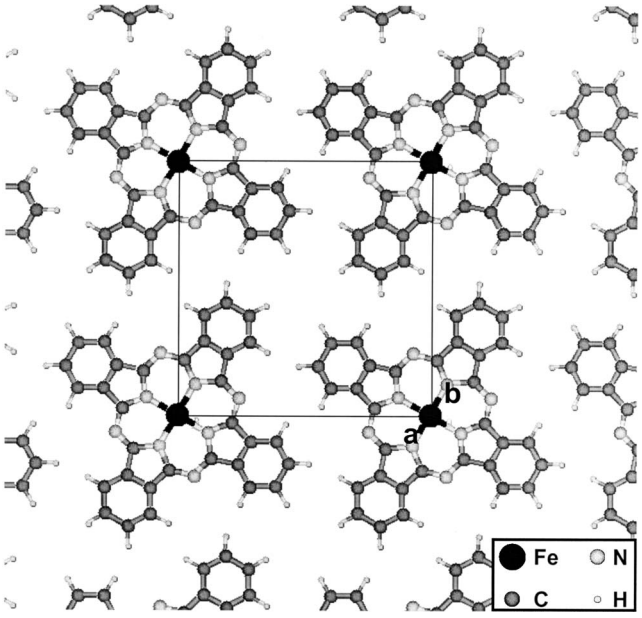

FIG. 7. Top down schematic of FePc monolayer. $a=b=13.7$ Å.

simulations since even FePc-FePc bonding leaves the NO chemisorption energy unchanged as discussed above. The optimized FePc monolayer film also has D_{4h} symmetry and simulated bond lengths and bond angles that agree with the values obtained for the simulated monomer to within 1%. The simulated chemisorption well depth for NO adsorption to the Fe metal of the FePc monolayer is nearly identical to that obtained for the monomer and trimer (−1.69 eV). NO binding results in an Fe–N(O) bond length of 1.73 Å and, like that observed in the monomer and trimer, the FePc molecule relaxes around the NO to give an N–Fe–N bond angle of 161°.

Chemisorption of NO onto the Fe metal of the FePc monolayer induces a change in its electronic structure similar to that observed in the FePc monomer and trimer. Figure 8 shows the Fe PDOS of the FePc monolayer before and after NO adsorption onto the Fe metal. The Fe PDOS of the monolayer contains a partially filled state at midgap and an unfilled state centered at 0.59 eV. When NO binds to the Fe metal of the FePc monolayer, the midgap Fe state is shifted into the filled state centered at −0.40 eV. The lowest energy unfilled Fe state is shifted from 0.59 eV to the higher energy state centered at 1.28 eV. The similarity in electronic structure changes upon NO adsorption to the metal of the FePc monolayer and monomer suggests that in-plane FePc-FePc interactions do not affect analyte binding to the metal center.

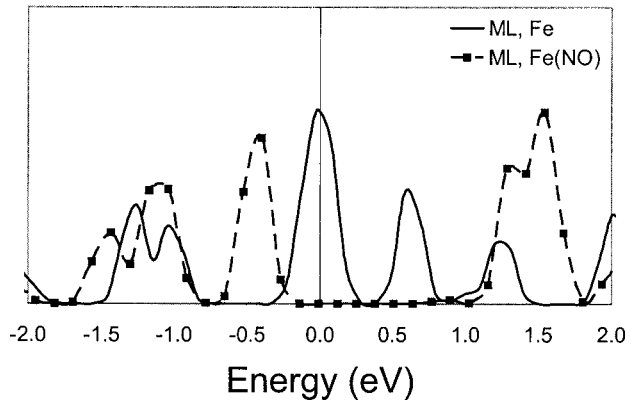

FIG. 8. Solid line represents Fe PDOS of the clean monolayer and solid squares represent Fe PDOS for NO adsorbed onto the Fe metal of the FePc monolayer. Since the DOS of the monolayer is similar to that observed for the monomer and trimer; the monolayer DOS is not shown.

Analysis of the atomic charges of the FePc monolayer before and after NO adsorption onto the Fe metal using the Bader charge distribution method shows that there is a transfer of charge between the adsorbate and FePc monolayer. When NO adsorbs onto the Fe metal, the Fe metal loses $0.25e^-$ while the NO molecule gains $0.26e^-$, consistent with experimental results showing an increase in current in *p*-type MPc films upon exposure to NO. These values are comparable to those observed in both the FePc monomer and trimer suggesting that in- and out-of-plane FePc-FePc interactions have a negligible effect on NO binding.

IV. CONCLUSIONS

Electron withdrawing (NO) and electron donating (NH_3) analyte binding to the metal center and aromatic rings of the FePc were investigated. The simulations show that NO strongly chemisorbs to the Fe metal center and physisorbs to all other nonmetal sites. Conversely, NH_3 only weakly chemisorbs to the Fe metal center. NO can undergo a barrierless migration from some of the physisorption sites to the deep chemisorption well on the iron metal center, consistent with molecular beam sticking measurements. PDOS simulations show that the binding of NO and NH_3 to the FePc metal center results in a transfer of charge between the Fe metal and analyte, consistent with multiple conductivity and sensor experiments. Simulations comparing the binding of NO to the FePc monomer, trimer, and monolayer films showed that both in- and out-of-plane FePc-FePc intermolecular interactions have a negligible effect on the FePc electronic structure and NO binding, suggesting that the FePc monomer is a sufficient model of the FePc film.

ACKNOWLEDGMENTS

The authors would like to thank AFOSR MURI F49620-02-1-0288 and NSF CHE-0350571 for funding for computational resources and the Department of Homeland Security for appointing Ngoc L. Tran to the U.S. Department of Homeland Security (DHS) Scholarship and Fellowship Program, administered by the Oak Ridge Institute for Science and Education (ORISE) through an interagency agreement between the U.S. Department of Energy (DOE) and DHS. ORISE is managed by Oak Ridge Associated Universities (ORAU) under DOE Contract No. DE-AC05-06OR23100.

[1] L. Lozzi, S. Santucci, and S. La Rosa, Appl. Phys. Lett. **88**, 133505 (2006).
[2] K. Nebesny, G. Collins, P. Lee, L. Chau, J. Danziger, E. Osburn, and N. Armstrong, Chem. Mater. **3**, 829 (1991).
[3] J. Buchholz and G. Somorjai, J. Chem. Phys. **66**, 573 (1977).
[4] X. Lu, K. Hipps, X. Wang, and U. Mazur, J. Am. Chem. Soc. **118**, 7197 (1996).
[5] X. Lu and K. Hipps, J. Phys. Chem. B **101**, 5391 (1997).
[6] T. Gopakumar, M. Lackinger, M. Hackert, F. Muller, and M. Hietschold,

J. Phys. Chem. B **108**, 7839 (2004).
[7] P. Day, Z. Wang, and R. Pachter, J. Mol. Struct.: THEOCHEM **455**, 33 (1998).
[8] M. Liao and S. Scheiner, J. Chem. Phys. **114**, 9780 (2001).
[9] V. Mastryukov, C. Ruan, M. Fink, Z. Wang, and R. Pachter, J. Mol. Struct. **556**, 225 (2000).
[10] J. Germain, A. Pauly, C. Maleysson, J. Blanc, and B. Schollhorn, Thin Solid Films **333**, 235 (1998).
[11] B. Schollhorn, J. Germain, A. Pauly, C. Maleysson, and J. Blanc, Thin Solid Films **326**, 245 (1998).
[12] T. Jones, B. Bott, and S. Thorpe, Sens. Actuators **17**, 467 (1989).
[13] H. Tada, H. Touda, M. Takada, and K. Matsushige, J. Porphyr. Phthalocyanines **3**, 667 (1999).
[14] N. Ishikawa, D. Maurice, and M. HeadGordon, Chem. Phys. Lett. **260**, 178 (1996).
[15] K. Nguyen and R. Pachter, J. Chem. Phys. **114**, 10757 (2001).
[16] L. Lozzi, S. Santucci, S. La Rosa, B. Delley, and S. Picozzi, J. Chem. Phys. **121**, 1883 (2004).
[17] T. Yamaguchi, J. Phys. Soc. Jpn. **66**, 749 (1997).
[18] B. Bialek and P. Bragiel, Acta Phys. Pol. **89**, 443 (1996).
[19] B. Szczepaniak and P. Bragiel, Vacuum **46**, 465 (1995).
[20] B. Bialek, Opt. Appl. **35**, 323 (2005).
[21] L. Lozzi, S. Picozzi, S. Santucci, C. Cantalini, and B. Delley, J. Electron Spectrosc. Relat. Phenom. **137–140**, 101 (2004).
[22] G. Kresse and J. Furthmuller, Comput. Mater. Sci. **6**, 15 (1996).
[23] G. Kresse and J. Furthmuller, Phys. Rev. B **54**, 11169 (1996).
[24] G. Kresse and J. Hafner, J. Phys.: Condens. Matter **6**, 8245 (1994).
[25] J. Perdew, K. Burke, and M. Ernzerhof, Phys. Rev. Lett. **77**, 3865 (1996).
[26] D. Vanderbilt, Phys. Rev. B **41**, 7892 (1990).
[27] J. Kirner, W. Dow, and W. Scheidt, Inorg. Chem. **15**, 1685 (1976).
[28] Y. Fu, Y. Mou, B.-L. Lin, L. Liu, and Q.-X. Guo, J. Phys. Chem. A **106**, 12386 (2002).
[29] C. I. Sainz-Diaz, J. Phys. Chem. A **106**, 6600 (2002).
[30] Y. Sadaoka, Y. Sakai, N. Yamazoe, and T. Seiyama, Denki Kagaku **50**, 457 (1982).
[31] P. Redhead, Vacuum **12**, 203 (1962).
[32] D. A. Becke, J. Chem. Phys. **96**, 2155 (1992).
[33] S. Bishop, N. Tran, G. Poon, and A. Kummel, J. Chem. Phys. **127**, 214702 (2007).
[34] Q. Zhou and R. Gould, Thin Solid Films **317**, 436 (1998).
[35] T. Nyokong and S. Vilakazi, Talanta **61**, 27 (2003).
[36] R. Collins and K. Mohammed, Thin Solid Films **145**, 133 (1986).
[37] D. E. Barlow, L. Scudiero, and K. W. Hipps, Langmuir **20**, 4413 (2004).
[38] R. Gould, Coord. Chem. Rev. **156**, 237 (1996).
[39] B. Bialek, I. Kim, and J. Lee, Surf. Sci. **526**, 367 (2003).
[40] Y. Lee, C. Hsiao, C. Chang, and Y. Yang, Sens. Actuators B **94**, 169 (2003).
[41] G. Henkelman, A. Arnaldsson, and H. Jonsson, Comput. Mater. Sci. **36**, 354 (2006).
[42] R. Collins and K. Mohammed, J. Phys. D **21**, 154 (1988).
[43] M. Ashida, N. Uyeda, and E. Suito, J. Cryst. Growth **8**, 45 (1971).